# Analysis of Finite Arrays—A New Approach

Boris Tomasic, *Senior Member, IEEE,* and Alexander Hessel, *Life Fellow, IEEE*

***Abstract*—A novel method for the analysis of finite arrays is presented. The method is based on a global array concept where the array problem (for single-mode elements) is reduced to a solution of a single Fredholm integral equation of the second kind. This formulation offers several types of solutions (not all explored yet) with illuminating results. The approximate solution of this integral equation, for example, yields finite array characteristics in terms of equivalent infinite array scattering parameters and mutual admittances. The method is general, i.e., applicable to any element-type and periodic array geometry. Presently, the method applies to single-mode elements (one unknown per element), however, it can be extended to a multimode analysis.**

***Index Terms*—Antenna arrays, finite phased arrays.**

## I. Introduction

PHASED-array antennas can be analyzed using two basic methods: an element-by-element approach and a periodic structure approach. The former method, which requires evaluation and inversion of a matrix, is rigorous and well suited for small array antennas [1]. However, it is often too complex and numerically/computationally difficult to apply to large finite arrays. The periodic structure approach [2], which usually is based on a unit cell concept, is a simple and approximate method that neglects the array edge effects and consequently is not sufficiently accurate for low sidelobe array designs. Beside these two basic methods, there are a number of techniques for analysis of finite large arrays [3]–[12]. Each of these techniques has advantages in particular applications; however, improvements in accuracy, generality, simplicity (theoretical and computational), and physical interpretation of the results are still desired.

This paper explores a new approach to the solution of finite arrays. The method presented has the accuracy of the element-by-element approach and the simplicity of the periodic structure approach. It is applicable to any single-mode element type and periodic array geometry. The method replaces the conventional solution of simultaneous integral equations, one for each element, by casting the discretized set of algebraic equations into a single (for single-mode elements) Fredholm-type integral equation of the second kind for a global generating function $\hat{V}$. The generating function $\hat{V}$ is called global because it gives a perspective on the array problem in the form of a single integral equation. The kernel of the integral equation is the product of the active admittance of the infinite array and the array factor of the uniformly illuminated finite array. Individual aperture voltages (or currents) are subsequently obtained by Fourier integral inversion.

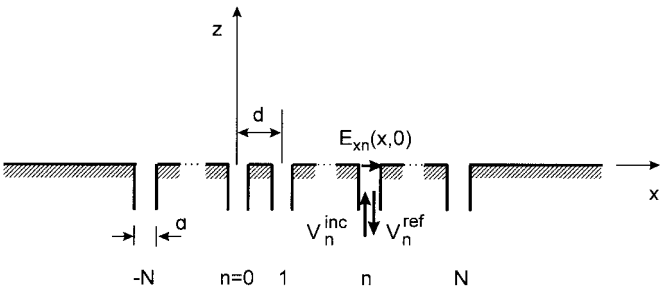


Fig. 1. Array geometry.

The appeal of the Fredholm integral equation formulation is that it is flexible, being amenable to many types of solutions, not all of which have been explored. For example:

1) since the kernel in the Fredholm integral equation is separable, the integral equation can be transformed into a linear system of equations, which is a well-known conventional representation;
2) the integral equation can be solved using variational techniques in conjunction with standard integration codes;
3) the integral equation can be solved using iterative schemes (In this case, the initial value for $\hat{V}$ can be chosen to be that of an equivalent infinite array. For large arrays, it is expected that only a few iterative steps will be needed for numerical evaluation of the Fredholm equation, thus the method is rapidly convergent.);
4) the Fredholm integral equation can also be solved approximately by taking advantage of the local property of the array factor in the kernel; the results are illuminating and, as will be shown, can be expressed in terms of infinite array coupling coefficients and mutual admittances.

## II. Derivation of the Integral Equation

The formal derivation of the Fredholm integral equation is given in Appendix A. Below we present an alternative derivation, the engineering approach, which results in the same integral equation.

### A. Array Model and Excitation

To demonstrate the basic concept we select a simple two-dimensional array of $2N+1$ equispaced "single-mode" elements shown in Fig. 1, where $d$ is the element spacing. The

Manuscript received June 2, 1997; revised June 11, 1998. This work was supported in part by the Air Force Office of Scientific Research under Project 2304I302.

B. Tomasic is with the Air Force Research Laboratory, Electromagnetics Technology Directorate, Hanscom AFB, MA 01701 USA.

A. Hessel, deceased, was with Polytechnic University, Farmingdale, NY 11735 USA.

Publisher Item Identifier S 0018-926X(99)04435-X.

array elements are parallel-plate-guide-fed slits, of width $a$ in a ground plane with a single TEM aperture field distribution. The elements are excited according to

$$V_n^{\text{inc}}(\delta) = V_0^{\text{inc}} e^{-jn\delta}, \qquad n = -N, \cdots, N \tag{1}$$

where $n$ denotes the element serial numbers, $\delta$ is the interelement phasing, and $V_n^{\text{inc}}$ are the TEM-mode incident voltages at $z = 0^-$ (aperture). The total voltage, $V_n$, in the aperture is, therefore, the sum of the incident and reflected voltages, i.e.,

$$V_n(\delta) = V_n^{\text{inc}}(\delta) + V_n^{\text{ref}}(\delta). \tag{2}$$

The objective of the analysis is to determine the $V_n$'s (with known $V_n^{\text{inc}}$'s) in a mutually coupled array environment.

### B. Modal Currents $I_n$—Network Representation

For an array with $2N+1$ elements excited with equal amplitude and progressive phase, in a single TEM-mode approximation the modal voltages $V_n(\delta)$ and modal currents $I_n(\delta)$ at $z = 0^-$ (aperture) are related by the mutual admittance matrix $\underline{\mathbf{Y}}^{\infty}$ as

$$\{I_n\} = \underline{\mathbf{Y}}^{\infty}\{V_n\} \tag{3a}$$

where the modal voltage and current vectors are

$$\{V_n\} = \begin{bmatrix} V_N \\ V_{N-1} \\ \vdots \\ V_n \\ \vdots \\ V_{-N} \end{bmatrix}, \qquad \{I_n\} = \begin{bmatrix} I_N \\ I_{N-1} \\ \vdots \\ I_n \\ \vdots \\ I_{-N} \end{bmatrix}. \tag{3b}$$

In (3a), $\underline{\mathbf{Y}}^{\infty}$ refers to an infinite array, however, since in single-mode approximation $V_n = 0$ for $|n| > N$, $\underline{\mathbf{Y}}^{\infty}$ is a $(2N+1) \times (2N+1)$ complex symmetric Toeplitz matrix.

To facilitate the analysis, we define the global generating function

$$\hat{V}(\nu, \delta) = \sum_{n=-N}^{N} V_n(\delta) e^{jn\nu} \tag{4a}$$

and thus

$$V_n(\delta) = \frac{1}{2\pi} \int_{-\pi}^{\pi} \hat{V}(\nu, \delta) e^{-jn\nu}\, d\nu \tag{4b}$$

or in vector form

$$\{V_n(\delta)\} = \frac{1}{2\pi} \int_{-\pi}^{\pi} \hat{V}(\nu, \delta)\{e^{-jn\nu}\}\, d\nu. \tag{4c}$$

Noting that

$$\underline{\mathbf{Y}}^{\infty}\{e^{-jn\nu}\} = Y^{\infty}(\nu)\{e^{-jn\nu}\} \tag{5a}$$

where $Y^{\infty}$ is the active admittance of an infinite array, substitution of (4c) into (3a) yields

$$\{I_n(\delta)\} = \frac{1}{2\pi} \int_{-\pi}^{\pi} Y^{\infty}(\nu)\hat{V}(\nu, \delta)\{e^{-jn\nu}\}\, d\nu. \tag{5b}$$

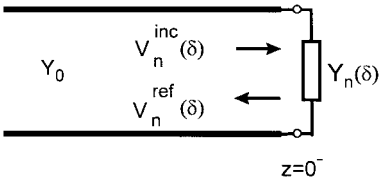


Fig. 2. Equivalent transmission line representation of parallel-plate-guide array element.

### C. Modal Currents $I_n$—Transmission Line Representation

In a parallel-plate waveguide at the aperture $(z = 0^-)$, the TEM-mode voltages and currents are (see Fig. 2)

$$V_n(\delta) = V_n^{\text{inc}}(\delta)[1 + \Gamma_n(\delta)] \tag{6a}$$

$$I_n(\delta) = Y_0 V_n^{\text{inc}}(\delta)[1 - \Gamma_n(\delta)] \tag{6b}$$

where the parallel-plate guide characteristic admittance is

$$Y_0 = \sqrt{\frac{\epsilon_0}{\mu_0}} = \frac{1}{376.7}\, S \tag{6c}$$

and $\Gamma_n$ is the active reflection coefficient of the finite array. From (6a)

$$\Gamma_n(\delta) = \frac{V_n(\delta)}{V_n^{\text{inc}}(\delta)} - 1 \tag{7a}$$

and, consequently,

$$I_n(\delta) = 2Y_0 V_n^{\text{inc}}(\delta) - Y_0 V_n(\delta), \qquad -N \le n \le N. \tag{7b}$$

### D. Integral Equation

Equating (5b) and (7b), we get

$$\frac{1}{2\pi} \int_{-\pi}^{\pi} Y^{\infty}(\nu)\hat{V}(\nu, \delta) e^{-jn\nu}\, d\nu = 2Y_0 V_n^{\text{inc}}(\delta) - Y_0 V_n(\delta). \tag{8}$$

Multiplying (8) by $e^{jn\alpha}$ and summing $\sum_{n=-N}^{N}$ yields an inhomogeneous Fredholm-type integral equation of the second kind

$$\hat{V}(\alpha, \delta) = C \int_{-\pi}^{\pi} K(\alpha, \nu)\hat{V}(\nu, \delta)\, d\nu + \mathcal{F}(\alpha, \delta) \tag{9a}$$

where the constant $C$ is

$$C = -\frac{1}{2\pi Y_0} \tag{9b}$$

and the kernel

$$K(\alpha, \nu) = Y^{\infty}(\nu) AF(\alpha, \nu). \tag{9c}$$

Here, as mentioned above, $Y^{\infty}$ is the active admittance of an equivalent infinite array and $AF$ is the array factor given by

$$AF(\alpha, \nu) = \sum_{n=-N}^{N} e^{jn(\alpha - \nu)}. \tag{10}$$

The inhomogeneous term in (9a) defines the array excitation and is

$$\mathcal{F}(\alpha, \delta) = 2 \sum_{n=-N}^{N} V_n^{\text{inc}}(\delta) e^{jn\alpha}. \tag{11}$$

Having solved for $\hat{V}$, we determine the total voltages in the apertures from (4b), i.e.,

$$V_n(\delta) = \frac{1}{2\pi}\int_{-\pi}^{\pi} \hat{V}(\alpha, \delta)e^{-jn\alpha}\,d\alpha, \qquad n = -N, \cdots, 0, \cdots, N. \tag{12}$$

It is interesting to note that since the kernel in integral equation (9a) is separable (degenerate), the integral equation can be transformed into a system of linear equations, which is a well-known conventional representation [13], [14].

## III. Solution of the Integral Equation

### A. Transformation of Variable

We seek a solution in the form

$$V_n(\delta) = V_n^{\infty}(\delta) + v_n(\delta) \tag{13}$$

where $V_n^{\infty}$ are the known voltages of the equivalent infinite array and $v_n$ represents the correction to an infinite array solution. Consequently

$$\hat{V}(\nu, \delta) = \hat{V}^{\infty}(\nu, \delta) + \hat{v}(\nu, \delta) \tag{14a}$$

where

$$\hat{V}^{\infty}(\nu, \delta) = \sum_{n=-N}^{N} V_n^{\infty}(\delta)e^{jn\nu} \tag{14b}$$

and

$$\hat{v}(\nu, \delta) = \sum_{n=-N}^{N} v_n(\delta)e^{jn\nu}. \tag{14c}$$

From (14c), the correction term is

$$v_\ell(\delta) = \frac{1}{2\pi}\int_{-\pi}^{\pi} \hat{v}(\alpha, \delta)e^{-j\ell\alpha}\,d\alpha, \qquad \ell = 0, \pm 1, \cdots, \pm N. \tag{15}$$

Substituting (14a) into (9a) we obtain the Fredholm integral equation for $\hat{v}$

$$\hat{v}(\alpha, \delta) = C\int_{-\pi}^{\pi} K(\alpha, \nu)\hat{v}(\nu, \delta)\,d\nu + f(\alpha, \delta) \tag{16a}$$

where

$$f(\alpha, \delta) = 2V_0^{inc}AF(\alpha, \delta) - \hat{V}^{\infty}(\alpha, \delta) + \mathcal{I}(\alpha, \delta) \tag{16b}$$

and

$$\mathcal{I}(\alpha, \delta) = C\int_{-\pi}^{\pi} K(\alpha, \nu)\hat{V}^{\infty}(\nu, \delta)\,d\nu \tag{16c}$$

are known functions.

### B. Approximate Solution

We consider an approximate solution of (16a). Note that for large arrays, the main contribution to the integral comes from the vicinity of the peak of the array factor, i.e., when $\nu = \alpha$. Thus, letting $N \to \infty$ in the expression for $AF$, (10), we obtain for the solution of (16a)

$$\hat{v}(\alpha, \delta) \simeq \frac{Y_0}{Y_0 + Y^{\infty}(\alpha)}\, f(\alpha, \delta). \tag{17}$$

Substitution of this expression into (15) yields $v_\ell$, in terms of known physical parameters of the infinite array. The details of the derivation can be found in [14]. Thus, we have

$$v_\ell(\delta) \simeq v_\ell^{(1)}(\delta) + v_\ell^{(2)}(\delta) \tag{18a}$$

where

$$v_\ell^{(1)}(\delta) = V_\ell^{inc}(\delta) - \frac{1}{2}V_\ell^{\infty}(\delta) - \frac{1}{2}\sum_{n'=-N}^{N}\frac{y_{\ell n'}}{Y_0}V_{n'}^{\infty}(\delta) \tag{18b}$$

and

$$v_\ell^{(2)}(\delta) = \sum_{n=-N}^{N} V_n^{inc}(\delta)S_{\ell n}^{\infty} - \tfrac{1}{2}\sum_{n=-N}^{N} V_n^{\infty}(\delta)S_{\ell n}^{\infty} - \frac{1}{2}\sum_{n=-N}^{N} S_{\ell n}^{\infty}\sum_{n'=-N}^{N}\frac{y_{nn'}}{Y_0}V_{n'}^{\infty}(\delta). \tag{18c}$$

Here, $y_{\ell n}$ are mutual admittances and $S_{\ell n}^{\infty}$ are scattering (coupling) coefficients of the corresponding infinite array. Having solved for the correction term $v_\ell$ (as already mentioned), the total voltage on the $\ell$th element of a finite array is

$$V_\ell(\delta) = V_\ell^{\infty}(\delta) + v_\ell(\delta) \tag{19}$$

where the total voltage of the corresponding infinite array $V_\ell^{\infty}$ is assumed to be known. As shown in [14], $v_\ell^{(1)} \to 0$ and $v_\ell^{(2)} \to 0$ as $N \to \infty$.

With known $V_\ell$'s, we readily derive other finite-array parameters. The active reflection coefficients $\Gamma_\ell$, for example, can be written in the following form [14]:

$$\Gamma_\ell(\delta) = \sum_{n=-N}^{N} S_{\ell n}^{\infty}e^{j(\ell-n)\delta} + \gamma_\ell^{c}(\delta), \qquad \ell = 0, \pm 1, \cdots, \pm N \tag{20a}$$

where the correction term $\gamma_\ell^c$ is

$$\gamma_\ell^{c}(\delta) \simeq \frac{1}{2}(1 + \Gamma^{\infty}(\delta))\left[2 - \left(1 + \sum_{n'=-N}^{N}\frac{y_{\ell n'}}{Y_0}\,e^{j(\ell-n')\delta}\right) - \sum_{n=-N}^{N} S_{\ell n}^{\infty}e^{j(\ell-n)\delta}\left(1 + \sum_{n'=-N}^{N}\frac{y_{nn'}}{Y_0}\,e^{j(n-n')\delta}\right)\right]. \tag{20b}$$

As shown in [14], the correction term $\gamma_\ell^c \to 0$ as $N \to \infty$. Neglecting the correction term, (20a) reduces to

$$\Gamma_\ell(\delta) \simeq \sum_{n=-N}^{N} S_{\ell n}^{\infty}e^{j(\ell-n)\delta} \tag{21}$$

which is a well-known expression for the active reflection coefficient of a finite array. This expression has often been used in practical array designs primarily because of its simplicity and reasonable accuracy.

### C. Single-Element Excitation

For the case of a single-element excitation, say element $p$, the previous analysis is also valid, where the inhomogeneous term in the Fredholm integral equation (9a) as given by (11) takes the form

$$\mathcal{F}(\alpha, p) = 2V_p^{\text{inc}} e^{jp\alpha}. \tag{22}$$

Thus, the integral equation (16a) for $\hat{v}(\alpha)$ remains the same and the inhomogeneous term is now

$$f(\alpha, p) = 2V_p^{\text{inc}} e^{jp\alpha} - \hat{V}^{\infty}(\alpha, p) + \mathcal{I}(\alpha, p) \tag{23a}$$

with

$$\hat{V}^{\infty}(\alpha, p) = \sum_{n=-N}^{N} V_n^{\infty}(p) e^{jn\alpha}. \tag{23b}$$

It is important to keep in mind that the $V_n^{\infty}$ in (23b) are now the total voltages in the apertures of the corresponding infinite array where element $p$ is excited with $V_p^{\text{inc}}$, and all other array elements are match terminated. Thus,

$$V_n^{\infty}(p) = V_p^{\text{inc}}(\delta_{np} + S_{np}^{\infty}) \tag{24a}$$

where the Kronecker delta is

$$\delta_{np} = \begin{cases} 1, & n = p \\ 0, & n \neq p. \end{cases} \tag{24b}$$

In view of (23), following the procedure of Section III-B, we find that the total aperture voltages are [14]

$$V_\ell(p) = V_\ell^{\infty}(p) + v_\ell(p) \tag{25a}$$

where the correction term to an infinite array solution is

$$v_\ell(p) \simeq v_\ell^{(1)}(p) + v_\ell^{(2)}(p) \tag{25b}$$

with

$$v_\ell^{(1)}(p) = V_p^{\text{inc}} \delta_{\ell p} - \tfrac{1}{2} V_\ell^{\infty}(p) - \frac{1}{2} \sum_{n'=-N}^{N} \frac{y_{\ell n'}}{Y_0} V_{n'}^{\infty}(p) \tag{25c}$$

and

$$v_\ell^{(2)}(p) = V_p^{\text{inc}} S_{\ell p}^{\infty} - \tfrac{1}{2} \sum_{n=-N}^{N} V_n^{\infty}(p) S_{\ell n}^{\infty} - \frac{1}{2} \sum_{n=-N}^{N} S_{\ell n}^{\infty} \sum_{n'=-N}^{N} \frac{y_{nn'}}{Y_0} V_{n'}^{\infty}(p). \tag{25d}$$

As in the active array case, $v_\ell^{(1)}(p) \to 0$ and $v_\ell^{(2)}(p) \to 0$ as $N \to \infty$ [14].

It is known that an active array solution can be obtained as a superposition of solutions due to individual element excitations in a match terminated array environment. Based on that, an alternative expression for the total aperture voltage of an active array (19) with excitation (1) can be simply written as

$$V_\ell(\delta) = \sum_{p=-N}^{N} V_\ell(p) \tag{26a}$$

where $V_\ell(p)$ is given by (25) with

$$V_p^{inc} = V_0^{\text{inc}} e^{-jp\delta}. \tag{26b}$$

At this point, we can also easily determine the scattering matrix of the finite array. To obtain the scattering coefficients, we divide both sides of (25) by $V_p^{\text{inc}}$. Therefore, from (25) using (24a) the scattering (coupling) coefficients between $p$th and $\ell$th elements (in a match-terminated array environment) are [14]

$$S_{\ell p} = S_{\ell p}^{\infty} + s_{\ell p} \tag{27a}$$

where the correction term is

$$s_{\ell p} \simeq s_{\ell p}^{(1)} + s_{\ell p}^{(2)} \tag{27b}$$

with

$$s_{\ell p}^{(1)} = \frac{1}{2}\delta_{\ell p} - \frac{1}{2} S_{\ell p}^{\infty} - \frac{1}{2} \sum_{n'=-N}^{N} (\delta_{n'p} + S_{n'p}^{\infty}) \frac{y_{\ell n'}}{Y_0} \tag{27c}$$

$$s_{\ell p}^{(2)} = S_{\ell p}^{\infty} - \tfrac{1}{2} \sum_{n=-N}^{N} (\delta_{np} + S_{np}^{\infty}) S_{\ell n}^{\infty} - \frac{1}{2} \sum_{n=-N}^{N} S_{\ell n}^{\infty} \sum_{n'=-N}^{N} (\delta_{n'p} + S_{n'p}^{\infty}) \frac{y_{nn'}}{Y_0}. \tag{27d}$$

As shown in [14],

$$s_{\ell p}^{(1)} \to 0 \quad \text{and} \quad s_{\ell p}^{(2)} \to 0 \quad \text{as} \quad N \to \infty. \tag{28}$$

### D. Graphical Interpretation of Coupling Mechanism

To observe the coupling mechanism in a finite array, from (27a) and (27b) we write

$$S_{\ell p} \simeq S_{\ell p}^{\infty} + s_{\ell p}^{(1)} + s_{\ell p}^{(2)}. \tag{29}$$

Furthermore, in view of (28), (27b), and (27c) can be rewritten in the following form [14]:

$$s_{\ell p}^{(1)} = \sum_{n}{}' S_{n'p}^{\infty} \frac{y_{\ell n'}}{2Y_0} \tag{30a}$$

$$s_{\ell p}^{(2)} = \sum_{n=-N}^{N} S_{\ell n}^{\infty} \sum_{n'}{}' S_{n'p}^{\infty} \frac{y_{nn'}}{2Y_0} \tag{30b}$$

where $\sum_{n'}{}' = \sum_{n'=N+1}^{\infty} + \sum_{n'=-(N+1)}^{-\infty}$ denotes the summation over elements outside of the actual array. Based on these expressions, coupling mechanism between array elements $p$ and $\ell$ can be graphically interpreted as follows. Suppose we excite element $p$ with $V_p^{\text{inc}} = 1$ V. According to (29) and (30) the received (and total) voltage in element $\ell$ is that of an equivalent infinite array $S_{\ell p}^{\infty}$ minus two contributions due to edge effects, i.e., $s_{\ell p}^{(1)}$ and $s_{\ell p}^{(2)}$. The $s_{\ell p}^{(1)}$ consists of an infinite number of terms, each representing a "single-bounce" coupling $S_{n'p}^{\infty} y_{\ell n'}/(2Y_0)$, as schematically shown in Fig. 3(a), where $n'$ is outside of the array. Similarly, $s_{\ell p}^{(2)}$ consists of an infinite number of "double-bounced" coupling

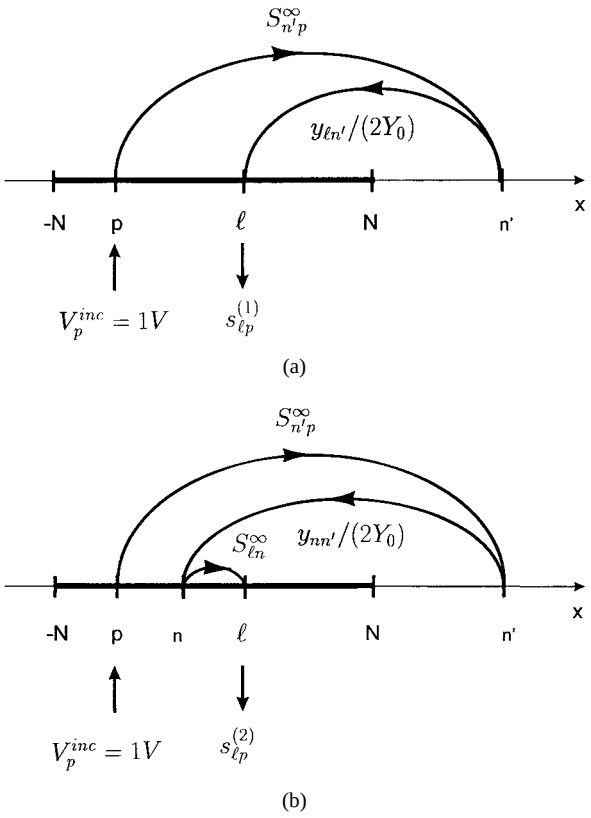


Fig. 3. Physical interpretation of coupling mechanism. (a) Single bounce. (b) Double bounce.

$S^{\infty}_{n'p} y_{nn'}/(2Y_0) S^{\infty}_{\ell n}$ where, as shown in Fig. 3(b), $n'$ is outside the array and $n$ is in the array region. From here we can deduce higher order terms in (29). However, as will be shown in the following section, the two-term solution is adequate for most practical applications.

## IV. Numerical Results

Numerical results obtained by our new approach were tested against an "exact" (reference) solution, which is obtained by a conventional method of moments (MoM) procedure briefly described in Appendix B. Results for the equivalent infinite array (derived in Appendix C) and results obtained by the approximation (21) are also shown. For clarity, in all figures below the exact results are shown by a solid line, infinite array results by a dashed line, results computed from (21) by hollow circles, and results of (our) new approach by solid filled circles.

As a first numerical example we selected a 25-element array with parallel plate guide width $a/\lambda = 0.2$, and element spacing $d/\lambda = 0.4$. The array elements are excited according to (1), i.e., with unit amplitude and linear phase progression $\delta$. Fig. 4(a) and (b) show the magnitude of the active reflection coefficients $|\Gamma_\ell|$ for the 25-element array at broadside scan ($\theta_0 = 0^0$). Specifically, Fig. 4(a) compares the infinite array solution for the active reflection coefficient with the exact solution. As is well known, the average of $|\Gamma_\ell|$ is determined by the infinite array solution, while oscillations about the average progressively increasing toward the edges are due to array edge effects. Also, this figure compares the finite array solution obtained from (21) with the exact solution. Notice

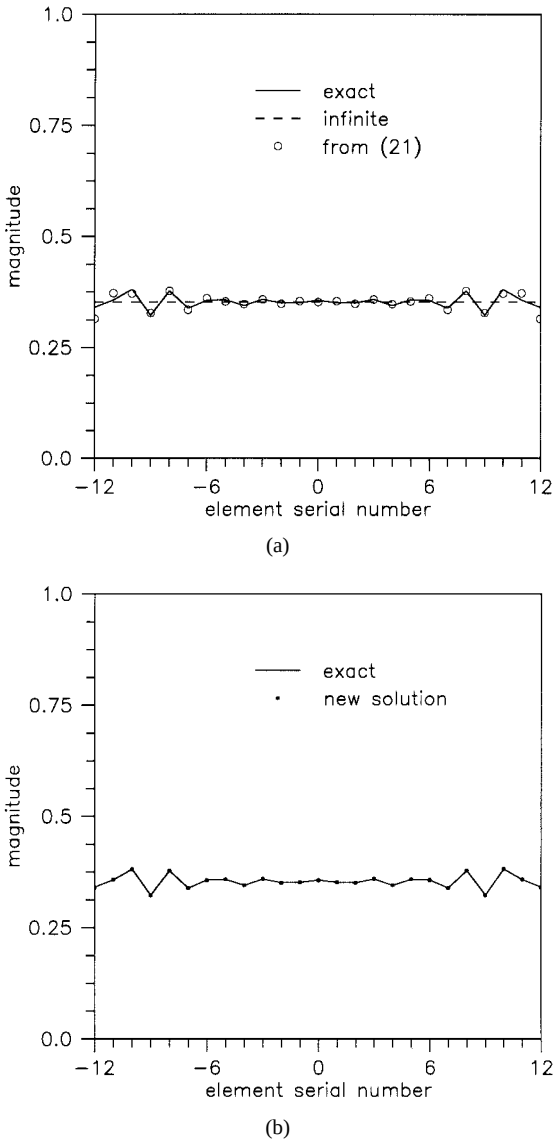


Fig. 4. Magnitude of active reflection coefficients for a 25-element array $\theta_0 = 0^0$. (a) Comparison between exact, infinite, and results obtained from (21). (b) Comparison between exact and our solution.

that except at the edges the agreement with the exact solution is quite good. Fig. 4(b) illustrates the finite array solution obtained from our new approach, which compares well with the exact results. Fig. 5(a) and (b) shows the same as Fig. 4(a) and (b), respectively, except that the scan angle $\theta_0 = 60°$.

For a second example we increased the array size to 51 elements. Fig. 6(a) and (b) compares the magnitude of the active reflection coefficients at broadside scan of an infinite array and results obtained by the new theory with the exact MoM solution. Fig. 7 shows a similar comparison when the array is scanned to $\theta_0 = 60°$. As seen, in both cases there is an excellent agreement between results obtained by the new approach and the conventional MoM-based reference solution.

The approximate solution to the Fredholm integral equation that we developed in Section III-B, was intended for large arrays. However, it turned out that the method also gives very good results for small arrays. To explain that, it is important to keep in mind that the approximate solution was

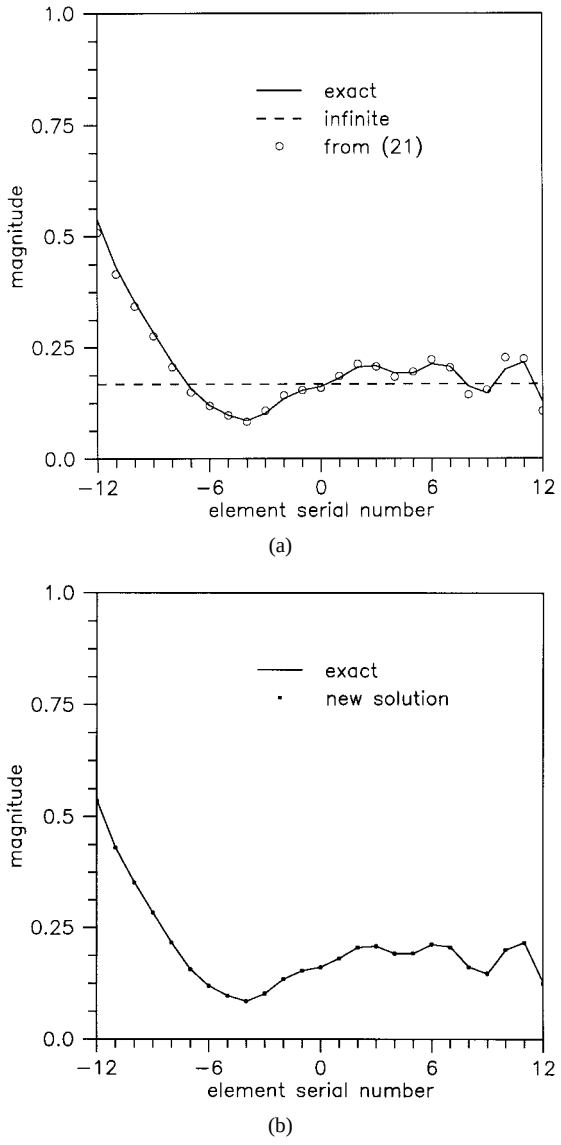


Fig. 5. Magnitude of active reflection coefficients for a 25-element array $\theta_0 = 60^0$. (a) Comparison between exact, infinite, and results obtained from (21). (b) Comparison between exact and our solution.

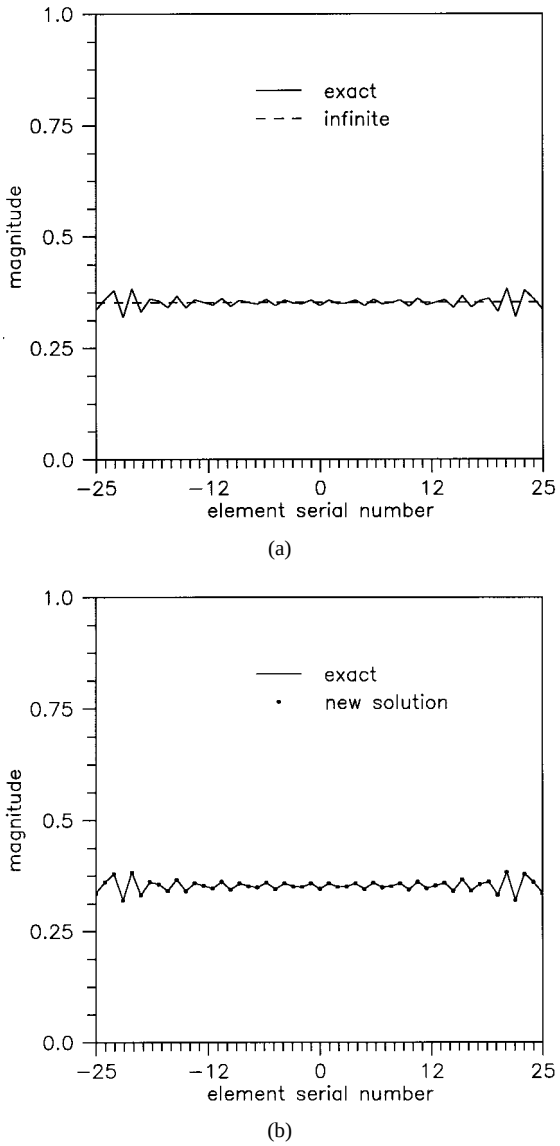


Fig. 6. Magnitude of active reflection coefficients for a 51-element array $\theta_0 = 0^0$. (a) Comparison between exact and infinite array results. (b) Comparison between exact and our solution.

obtained based on the fact that the main contribution to the integral in (16a) came from the vicinity of the peak of the array factor in the kernel of the Fredholm integral equation. The array factor, which is a sinc function, was approximated by a $\delta$-function. Thus for larger $N$, this approximation is better and as $N \to \infty$ the solution becomes exact. On the other hand, let us examine the rest of the integrand in (16a), i.e., $Y^{\infty}(\nu)\hat{v}(\nu)$. The active admittance of an infinite array, $Y^{\infty}(\nu)$ is a relatively slowly varying function of $\nu$ and $N$. However, the correction term $\hat{v}(\nu)$ is an oscillating function of $\nu$ with a period of approximately $4\pi/(2N+1)$. Therefore, the behavior of $Y^{\infty}(\nu)\hat{v}(\nu)$ is predominantly determined by the behavior of $\hat{v}(\nu)$. Since, the null-to-null beamwidth in the array factor is also $4\pi/(2N+1)$, we concluded that there is always about one oscillation of $Y^{\infty}(\nu)\hat{v}(\nu)$ per null-to-null beamwidth independent of $N$. Consequently, the error due to the $\delta$-function approximation for the array factor in the approximate solution is almost independent of the number of array elements $2N+1$. To demonstrate this, Fig. 8 shows the magnitude of the active reflection coefficients for a three-element array at $\theta_0 = 60°$ scan. The four data curves compare the solutions for the infinite array case, the approximation (21), the new theory and exact MoM.

To observe the grating lobe effects on the accuracy of the approximate solution, we also tested our theory on arrays with element spacings greater than $\lambda/2$. Fig. 9(a) and (b) shows the magnitude of the active reflection coefficients for a 13-element array with element spacing $d/\lambda = 0.6$ and parallel-plate-guide width $a/\lambda = 0.4$. In Fig. 9(a), the scan angle $\theta_0 = 42°$, which corresponds to a main beam location 42° off broadside and the grating lobe at endfire. Fig. 9(b) shows the same except that the main beam is at $\theta_0 = 60°$ while the grating lobe is in visible space. As seen in both cases, there is an excellent agreement between our results and the reference MoM results from which we concluded that our approximate solution is also accurate in the presence of grating lobes.

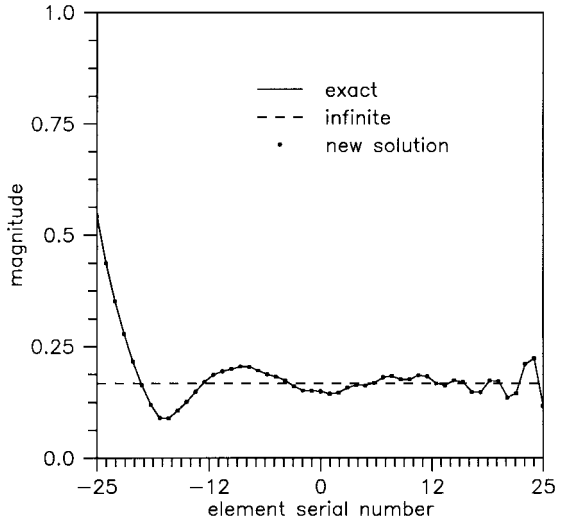


Fig. 7. Magnitude of active reflection coefficients for a 51-element array $\theta_0 = 60^0$ comparison between exact, infinite, and our results.

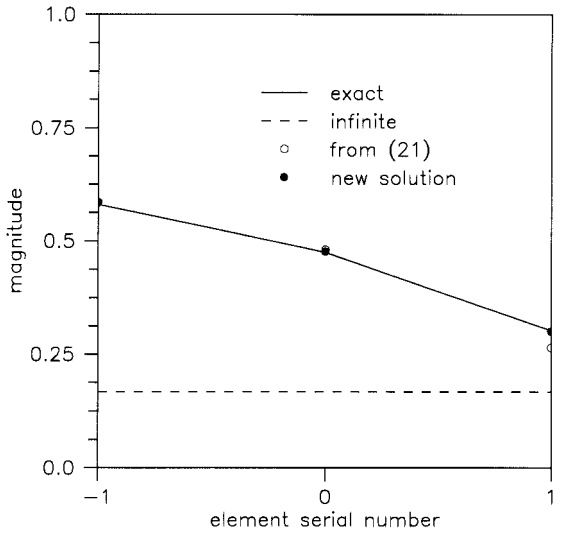


Fig. 8. Magnitude of active reflection coefficients for a three-element array, $\theta_0 = 60^0$, comparison between exact, infinite, those obtained from (21), and our results.

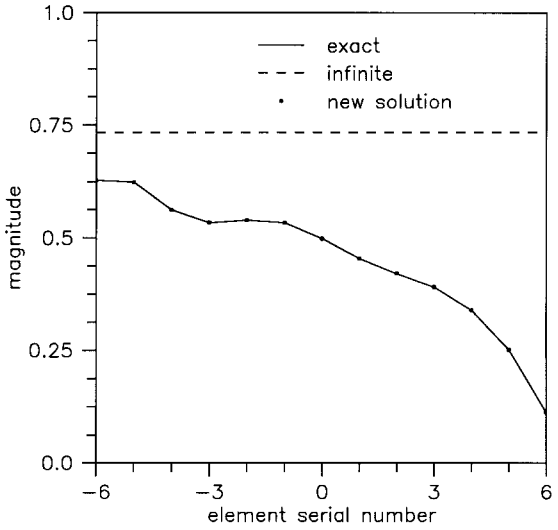


(a)

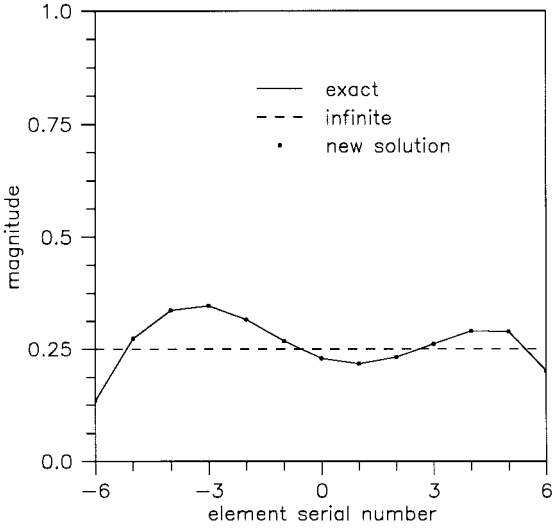


(b)

Fig. 9. Magnitude of active reflection coefficients for a 13-element array, comparison between exact, infinite, and our results. (a) $\theta_0 = 42^0$. (b) $\theta_0 = 60^0$.

For a single-element excitation in a match-terminated array, in Fig. 10(a) and (b) we compare the magnitude of the total voltages in the apertures calculated from (27) with the reference solution. The array consists of 13 elements with $a/\lambda = 0.2$ and $d/\lambda = 0.4$. In Fig. 10(a) the center array element is excited with $V_0^{\text{inc}} = 1$ V while in Fig. 10(b) the edge element is excited with $V_6^{\text{inc}} = 1$ V. To reduce the size of the plots for the excited elements, only $|V_0^{\text{ref}}|$ and $|V_6^{\text{ref}}|$ are shown. The respective voltages of an equivalent infinite array are also shown in these figures.

## V. Conclusions

A new method for the analysis of finite arrays has been developed. It replaces the conventional solution of simultaneous integral equations—one for each element by a single Fredholm-type integral equation of the second kind. This formulation offers new types of solutions, not all of which have been investigated. We have presented one approximate solution of this integral equation, which gives finite array characteristics in terms of the equivalent, infinite array-scattering parameters and mutual admittances. The method presently applies to single-mode elements and numerical agreement with exact MoM single-mode solutions has been shown to be excellent. In addition, unlike the element-by-element integral equation approach, this solution leads naturally to a physical interpretation of the coupling mechanism. The method can be extended to more realistic three-dimensional arrays and multimode elements.

## Appendix A
## Formal Derivation of the Integral Equation

### A. Fields in the Region $z \leq 0$

With reference to Fig. 1, the fields in the $n$th aperture (at $z = 0^-$) can be expressed in terms of the parallel plate

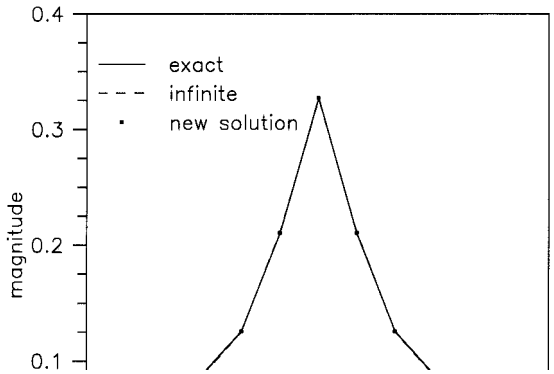
0.4
0.3
0.2
0.1
magnitude
exact
infinite
new solution